Radiology

Pitfalls in Liver Imaging[1]

Valérie Vilgrain, MD, PhD
Matthieu Lagadec, MD
Maxime Ronot, MD, PhD

Despite various sophisticated imaging techniques, there are numerous pitfalls in liver imaging. This review for residents discusses the major traps in image interpretation and gives some diagnostic clues to confidently interpret computed tomographic or magnetic resonance imaging studies.

Online supplemental material is available for this article.

Online SA-CME
See www.rsna.org/education/search/ry

Learning Objectives:

After reading the article and taking the test, the reader will be able to:

- Identify the main mimickers of cirrhosis
- Identify the main mimickers of liver tumors
- Describe the determinant of liver trophicity

Accreditation and Designation Statement

The RSNA is accredited by the Accreditation Council for Continuing Medical Education (ACCME) to provide continuing medical education for physicians. The RSNA designates this journal-based SA-CME activity for a maximum of 1.0 *AMA PRA Category 1 Credit™*. Physicians should claim only the credit commensurate with the extent of their participation in the activity.

Disclosure Statement

The ACCME requires that the RSNA, as an accredited provider of CME, obtain signed disclosure statements from the authors, editors, and reviewers for this activity. For this journal-based CME activity, author disclosures are listed at the end of this article.

[1] From the Université Paris Diderot, Sorbonne Paris Cité, Paris, France; INSERM 1149, CRI, Paris France; and Department of Radiology, APHP Hôpital Beaujon, 100 bd du Général Leclerc, 92110 Clichy, France. Received November 22, 2014; revision requested January 1, 2015; revision received January 20; accepted January 30; final version accepted February 24. **Address correspondence to** V.V. (e-mail: *valerie.vilgrain@bjn.aphp.fr*).

The liver is a tricky organ for radiologists. The external structure (lobes separated by the falciform ligament) does not reflect the internal structure, which has been clearly described by the anatomist Charles Couinaud. Besides the complex anatomy and the anatomic variants, which will not be considered in this review, there are several pitfalls to be avoided during liver imaging. Cirrhosis is the most common chronic liver disease but certain other liver diseases may have a pseudocirrhotic appearance at imaging and require different management. The differentiation of true liver tumors from pseudotumors can be challenging.

The goal of this review is to familiarize radiology residents and other practitioners with the most common pitfalls of liver imaging and to provide some diagnostic clues to confidently interpret computed tomographic (CT) or magnetic resonance (MR) imaging results. Three major topics will be discussed throughout the article. Morphologic changes of the liver are important imaging features for the diagnosis of cirrhosis. However, some other conditions can mimic cirrhosis, and this review highlights the most common differential diagnoses with imaging clues. The diagnosis of a tumor is based on clinical background, imaging characteristics, and the organ in which the tumor arises. As the origin of large abdominal tumors can be difficult to assess, we have thought it could be important to describe the imaging features that are most useful in making this determination. Last, liver lesions might be true tumors with proliferative activity, or they might be pseudotumors or pseudolesions, which are often treated conservatively. This review details important differential diagnoses of true liver tumors, the most common being focal fat deposition or focal sparing and perfusion disorders.

Essentials

- The majority of the noncirrhotic liver diseases, which mimic cirrhosis, are of vascular or biliary origin.
- Careful analysis of the large intra- and extrahepatic vessels is helpful to assess whether a large tumor originates from within the liver or outside it.
- The most common pseudolesions in liver segment 4 are related to focal fatty sparing or focal steatosis.

The Mimics of Cirrhosis

Cirrhosis is pathologically defined as multiple regenerative nodules surrounded by fibrous tissue. It is the end-stage disease of liver fibrosis, which may be the consequence of several chronic liver diseases. Although noninvasive imaging tests have been developed to diagnose and stage liver fibrosis, many patients are only diagnosed at a late stage, when they already have cirrhosis.

There are various imaging criteria for the diagnosis of cirrhosis, including a nodular liver surface, morphologic changes in the liver, and signs of portal hypertension. The morphologic changes associated with liver cirrhosis include atrophy of the right liver and segment 4, hypertrophy of the left liver lobe and the caudate lobe, increased fat in the porta hepatis, and expansion of the gallbladder fossa (1).

However, other noncirrhotic liver conditions can lead to morphologic changes in the liver that mimic cirrhosis. These changes may be due to obstruction of the major portal or hepatic veins, biliary obstruction, or more diffuse noncirrhotic chronic liver diseases.

Venous or Biliary Obstruction

The association between hepatic lobar atrophy and ipsilateral portal vein obstruction is well known and has been described in patients with isolated portal vein obstruction (Fig 1) or those with cholangiocarcinoma, resulting in both portal vein and biliary obstruction (2). Further details are shown in Figure E1 (online). In the latter, portal vein obstruction seems to be the dominant factor in the development of lobar atrophy. Atrophy of the area involved is associated with compensatory hypertrophy and/or hyperplasia of the nonaffected liver (atrophy-hypertrophy complex) (3). Interestingly, an experimental model has shown that the contralateral liver begins regeneration before the blood flow–deprived liver atrophies (4). Early changes are explained by the activation of multiple factors including proto-oncogenes (4). Biliary obstruction may also induce ipsilateral liver atrophy, especially if it is chronic, but this is usually less pronounced than the combination of portal vein and biliary obstruction. Unlike portal vein obstruction, isolated biliary obstruction does not seem to cause contralateral hypertrophy. Finally, hepatic venous obstruction is associated with ipsilateral liver atrophy (5). During obstruction of the major portal branch, hepatic vein, or intrahepatic bile ducts, besides ipsilateral atrophy imaging findings may show direct signs of vascular or biliary obstruction which are often associated with perfusion disorders. In particular, increased enhancement of the obstructed liver on arterial-phase contrast material–enhanced images is highly suggestive of portal venous obstruction. Both direct and indirect signs of obstruction (liver atrophy and perfusion disorders) make the diagnosis easy. The Table summarizes the most common imaging findings associated with portal vein, bile duct, or hepatic venous obstruction.

Diffuse Noncirrhotic Chronic Liver Diseases

Morphologic changes of the liver mimicking cirrhosis are present in several noncirrhotic liver diseases, most of them of vascular or biliary origin.

Cavernous transformation of the portal vein occurs as a result of com-

Published online
10.1148/radiol.2015142576 **Content codes:** GI CT MR

Radiology 2016; 278:34–51

Abbreviations:
GRE = gradient echo
IVC = inferior vena cava
MIP = maximum intensity projection
SE = spin echo

Conflicts of interest are listed at the end of this article.

Figure 1

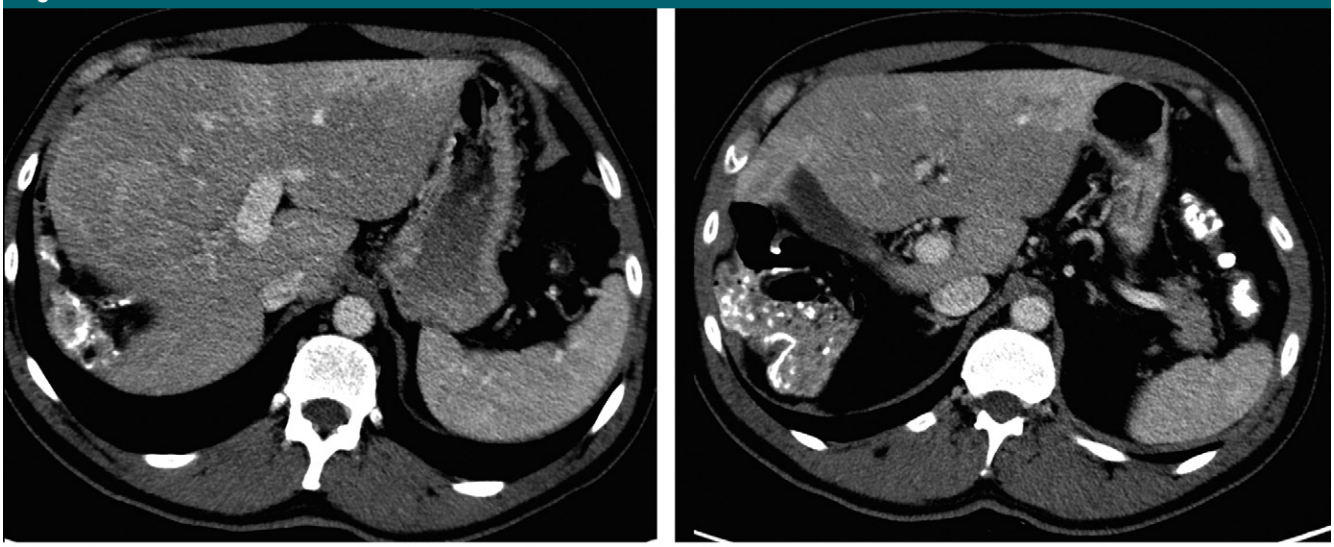

a. b.

Figure 1: Axial contrast-enhanced CT images in a 49-year-old man with marked atrophy of the right liver due to complete obstruction of the right portal vein. **(a, b)** Portal venous phase images obtained at different levels show right atrophy with displacement of the gallbladder.

The Most Common Imaging Findings Associated with Biliary, Portal Venous, or Hepatic Venous Obstruction

Finding	Biliary Obstruction	Portal Venous Obstruction	Hepatic Venous Obstruction
Ipsilateral atrophy	Marked if biliary obstruction is complete and chronic	Marked	Marked and related to hepatic venous anatomy
Contralateral hypertrophy	Present especially when associated with portal venous obstruction	Present	Present Hypertrophy of the caudate lobe can be seen
Biliary dilatation	Major	Absent	Absent
Liver enhancement at contrast-enhanced arterial phase imaging	Slightly increased in marked bile ducts dilatation	Increased	Same as contralateral lobe
Liver enhancement at contrast-enhanced portal venous phase imaging	Same as contralateral lobe	Same as contralateral lobe	Reticular or mosaic pattern can be seen

plete extrahepatic portal vein obstruction and is seen as multiple collateral veins in the porta hepatis. Atrophy of the right liver, hypertrophy of the caudate lobe, and signs of portal hypertension are confusing and can mimic cirrhosis. However the atrophy-hypertrophy complex is different from cirrhosis because hypertrophy is central (segment 4 and the caudate lobe) (Fig 2) as a result of maintained portal inflow and peripheral atrophy (right liver and left liver lobe) (6). Moreover, nodularity of the hepatic contour is usually not present (6). Imaging features also include direct signs of complete portal vein obstruction with lack of enhancement of the main portal vein and venous collaterals in the porta hepatis on contrast-enhanced CT and MR images.

Budd-Chiari syndrome is characterized by hepatic venous outflow obstruction in the absence of right-sided heart failure or constrictive pericarditis, which occurs in the small or large hepatic veins or the suprahepatic portion of the inferior vena cava (IVC). Approximately one-half of primary Budd-Chiari syndrome patients have myeloproliferative disorders. Other acquired and inherited conditions may be present and there is often a combination of causes in the same patient (7). Simultaneous venous involvement in all hepatic veins is rare, and a key finding is the morphologic changes of the liver with the atrophy-hypertrophy complex. As mentioned above, hepatic venous obstruction can result in ipsilateral atrophy. On the other hand, adaptive mechanisms include the development of a collateral hepatic venovenous circulation to divert the outflow circulation by bypassing the obstruction and connecting blocked territories to contiguous, well-drained territories. Thus, atrophy will appear in the obstructed liver segments and hypertrophy will be seen in

Figure 2

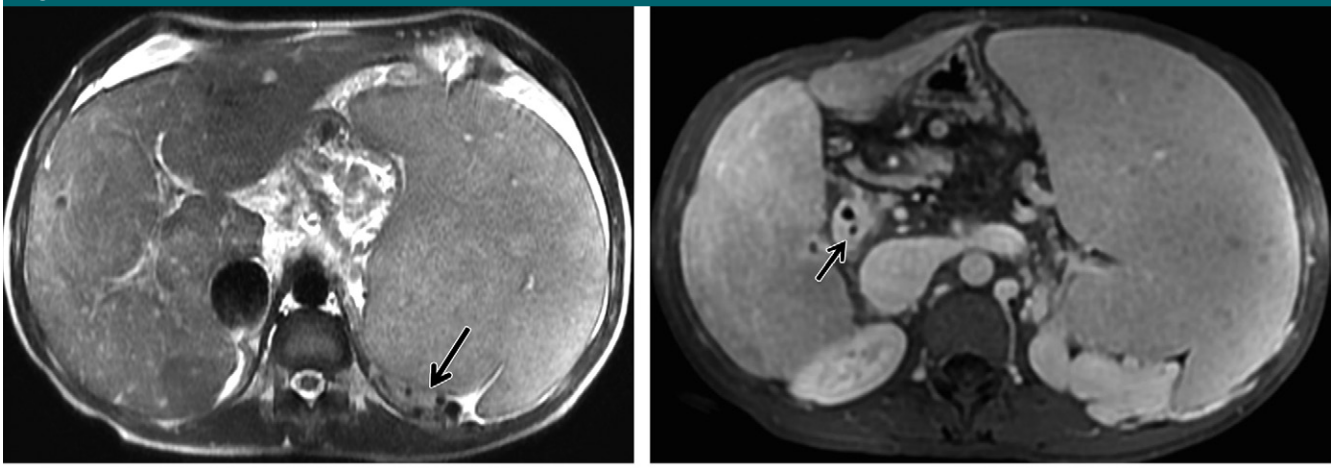

a. b.

Figure 2: MR images in a 27-year-old woman with morphologic changes of the liver secondary to cavernous transformation of the portal vein. **(a)** Fat-suppressed fast spin-echo (SE) T2-weighted image (repetition time msec/echo time msec, 2500–8000/90; flip angle, 90°; section thickness, 4 mm) shows central liver hypertrophy (segment 4 and caudate lobe), peripheral atrophy, and signs of portal hypertension (splenomegaly and portocaval collaterals [arrow]). **(b)** Contrast-enhanced gradient-echo (GRE) T1-weighted image (4.5/2.2; flip angle, 10°; section thickness, 4 mm) at the portal venous phase demonstrates portal cavernoma around the common bile duct (arrow).

liver segments where hepatic venous outflow is not altered. In most cases the caudate lobe is preserved and hypertrophic because most of the outflow of the caudate lobe is independent of the major hepatic veins and composed of many small veins that drain directly into the IVC (Fig 3). Hypertrophy of the caudate lobe is not specific for Budd-Chiari syndrome and may be seen in cirrhosis and other chronic liver diseases in association with splenomegaly and signs of portal hypertension. The diagnosis of Budd-Chiari syndrome is further supported by visualization of direct anomalies of the hepatic veins and the collateral circulation. Liver enhancement is often heterogeneous with a mottled appearance, and delayed enhancement in the periphery of the liver and around the hepatic veins is a typical feature. Nevertheless, chronic Budd-Chiari syndrome may be difficult to differentiate from cirrhosis (8).

Congenital hepatic fibrosis is a developmental malformation that belongs to the family of hepatic ductal plate malformations, resulting in a persistent additional embryonic bile duct structure in the portal tracts. Congenital hepatic fibrosis is usually associated with autosomal recessive polycystic kidney diseases, which together represent the most common hepatorenal fibrocystic diseases. Although they are usually diagnosed during childhood, it is not uncommon to first diagnose them in adult patients. The causative gene, *PKHD1*, encodes fibrocystin (polyductin) that localizes to the primary cilium, explaining why they are now called ciliopathies. The most common complication of congenital hepatic fibrosis is portal hypertension. Morphologic abnormalities of the liver (segmental hypertrophy or atrophy) are found in most patients, most frequently atrophy of the right liver and hypertrophy of the left liver lobe and the caudate lobe mimicking cirrhosis. Interestingly, segment 4 is normal sized or enlarged (9). Besides the morphologic changes of the liver, other abnormalities such as renal and biliary disorders that are not found in patients with cirrhosis are highly suggestive of this diagnosis. Biliary abnormalities include isolated common bile duct dilatation, Caroli syndrome, and dilatation of peripheral intrahepatic bile ducts, which usually can only be detected with MR cholangiopancreatography (Fig 4) (10). Further details are shown in Figure E2 (online).

Obliterative portal venopathy, also known as idiopathic portal hypertension and hepatoportal sclerosis, is one of the diseases that most closely mimics cirrhosis because portal hypertension is a key finding and in advanced cases, the imaging findings of liver nodularity and atrophy are indistinguishable from those of cirrhosis (11). This explains the series of patients who were considered to have cirrhosis and were diagnosed with obliterative portal venopathy at the pathologic assessment of liver explants (12). Obliterative portal venopathy is characterized by portal tract abnormalities showing thrombosis, fibrosis, and sclerosis. This disease also includes a spectrum of entities, such as nodular regenerative hyperplasia. Most patients manifest morphologic changes in the liver and in 25% of the cases they are similar to those observed in cirrhosis (atrophy of segment 4 and hypertrophy of caudate lobe). Fortunately, certain findings help differentiate between obliterative portal venopathy and cirrhosis: intra- or extrahepatic portal vein anomalies (acute or chronic, complete or partial obstruction, stenosis

Figure 3

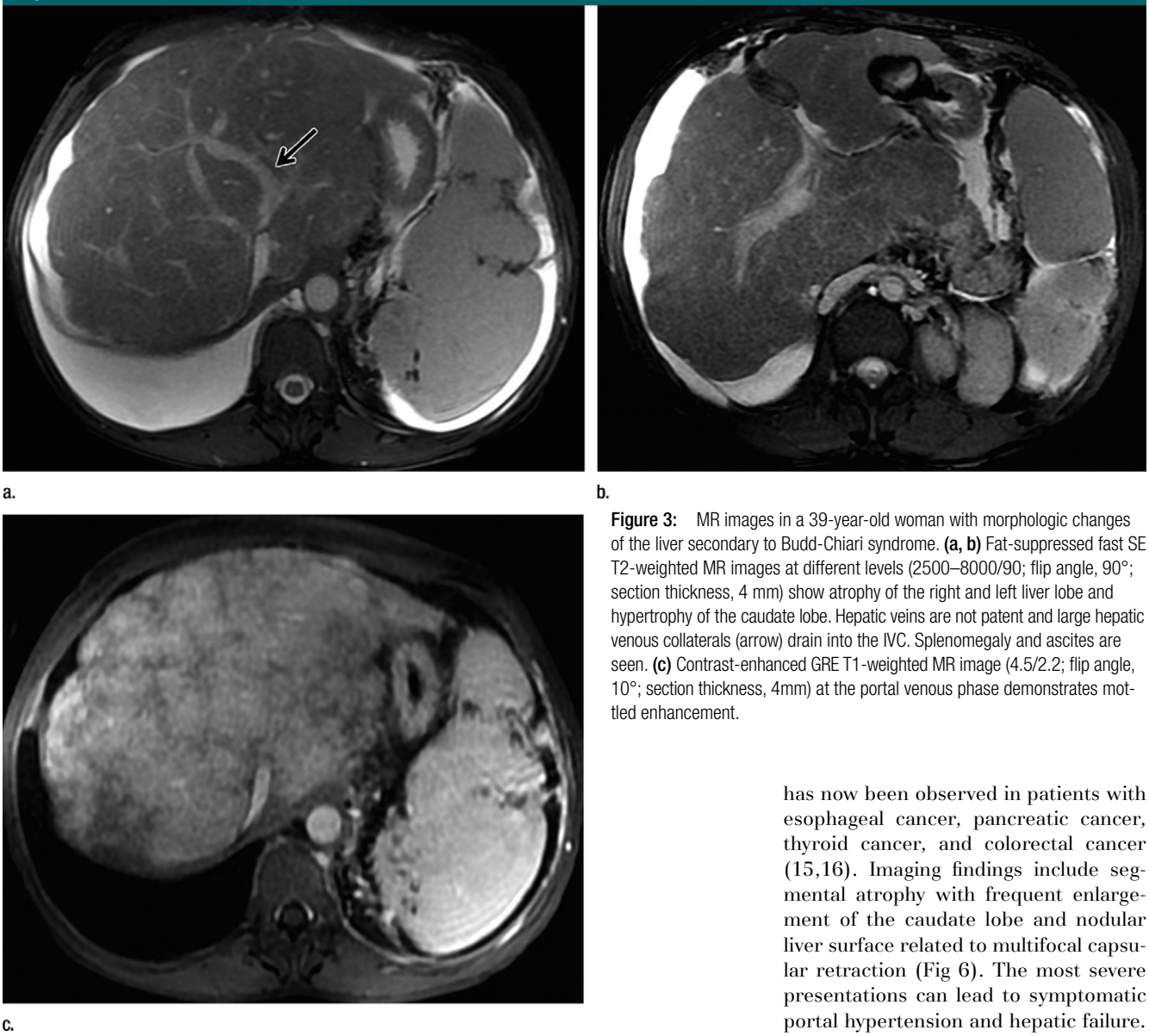

Figure 3: MR images in a 39-year-old woman with morphologic changes of the liver secondary to Budd-Chiari syndrome. **(a, b)** Fat-suppressed fast SE T2-weighted MR images at different levels (2500–8000/90; flip angle, 90°; section thickness, 4 mm) show atrophy of the right and left liver lobe and hypertrophy of the caudate lobe. Hepatic veins are not patent and large hepatic venous collaterals (arrow) drain into the IVC. Splenomegaly and ascites are seen. **(c)** Contrast-enhanced GRE T1-weighted MR image (4.5/2.2; flip angle, 10°; section thickness, 4mm) at the portal venous phase demonstrates mottled enhancement.

or lack of visibility and mural calcifications) (Fig 5) are mainly observed in patients with obliterative portal venopathy, whereas a nodular liver surface is rarely found (13). Further details are shown in Figure E3 (online).

Diffuse morphologic changes of the liver may also be found in patients with liver metastases (14). This condition is called "hepar lobatum" or more recently pseudocirrhosis. Although this entity can develop in the absence of chemotherapy, it clearly seems to be commonly associated with chemotherapy. The mechanism has not yet been elucidated. It could be due to tumor shrinkage and subsequent severe desmoplastic fibrosis around the liver metastases or nodular regenerative hyperplasia in response to chemotherapy. Interestingly, it is often observed in patients with a major morphologic response to chemotherapy (15). While it was initially described almost exclusively in patients with liver metastases from breast cancer, pseudocirrhosis has now been observed in patients with esophageal cancer, pancreatic cancer, thyroid cancer, and colorectal cancer (15,16). Imaging findings include segmental atrophy with frequent enlargement of the caudate lobe and nodular liver surface related to multifocal capsular retraction (Fig 6). The most severe presentations can lead to symptomatic portal hypertension and hepatic failure. The key to the diagnosis is a clinical history and normal liver imaging results at prior examinations. In a series of patients with breast cancer liver metastases who received chemotherapy, 75% had various degrees of liver contour abnormalities, from limited retraction to diffuse nodularity (17). Moreover, 9% of these patients developed portal hypertension. These changes may develop rapidly after a median follow-up of 15 months. Radiologists should be aware of this entity because in these patients anticancer therapy should be modified

Figure 4

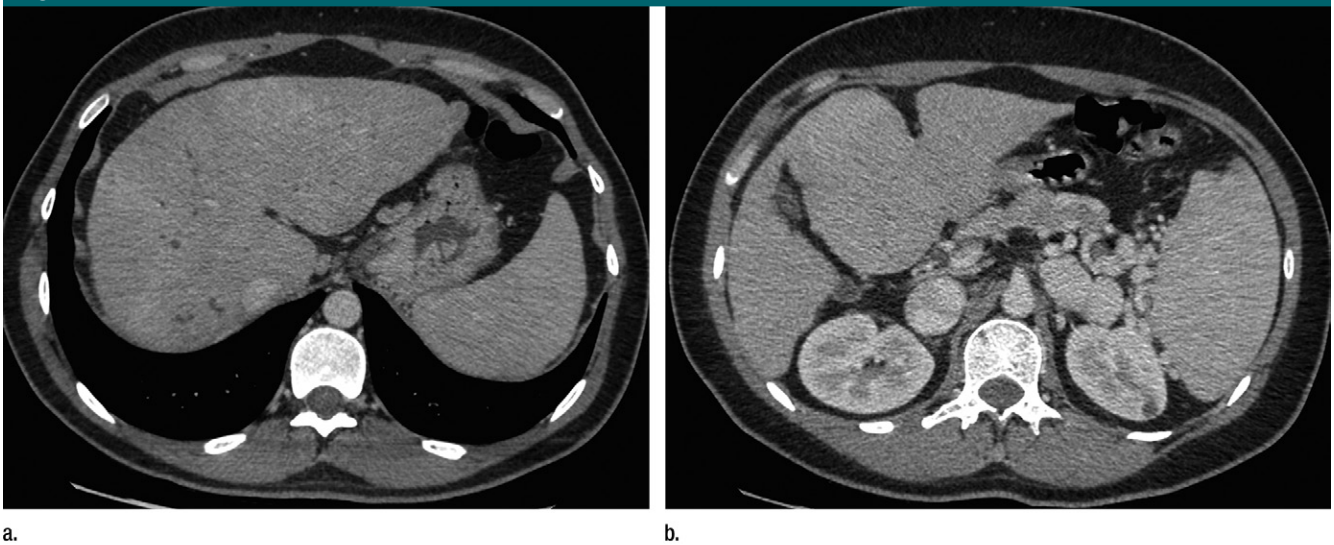

a. b.

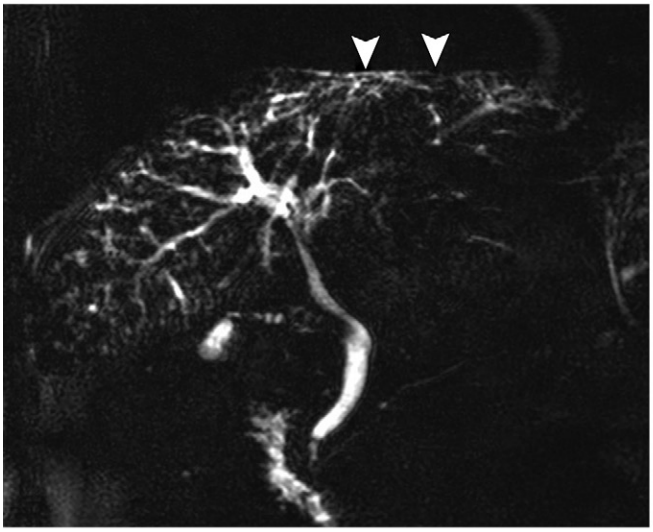

c.

Figure 4: Images in a 30-year-old man with morphologic changes of the liver secondary to congenital hepatic fibrosis. **(a, b)** Axial contrast-enhanced CT images at the portal venous phase show right atrophy with hypertrophy of segment 4 and the caudate lobe. Signs of portal hypertension are seen (splenomegaly and portocaval collaterals). **(c)** Image obtained at MR cholangiopancreatography (repetition time not applicable; echo time 909 msec; flip angle, 90°; section thickness, 20 mm) demonstrates slight dilatation of peripheral bile ducts (arrowheads).

and sometimes interrupted (16). The imaging findings in pseudocirrhosis have been shown to completely resolve in some patients (16).

Acute liver failure, a very severe disease with a high risk of spontaneous mortality, is characterized by the onset of hepatic encephalopathy from severe acute liver injury in the absence of pre-existing liver disease. The prognosis has dramatically changed with orthotopic liver transplantation, so it is crucial to assess the absence of chronic liver disease in these patients. Biopsy is often contraindicated as the patients commonly have abnormal blood liver tests and low platelet and coagulation factors. Unfortunately imaging findings can mimic cirrhosis. Portal hypertension is seen in most patients with acute liver injury, and ascites is the most common finding. Even more confusing, liver atrophy and liver surface nodularity (up to 43%) can be seen in these patients especially in those who have been ill for more than 7 days (18,19). This is thought to be due to confluent regenerative nodules and massive necrosis. Indeed, both radiologists and hepatologists should be aware of this and be careful not to misdiagnose cirrhosis because patients with acute liver failure can receive higher priority on transplantation waiting lists. On the other hand, incorrect prioritization (listing a patient as having fulminant hepatic failure whose explant is shown to have underlying cirrhosis) can have serious consequences for an institution, which can lose its UNOS (United Network for Organ Sharing) accreditation (19). The clinical background, a negative hepatitis B or C virus serology, or no history of alcohol abuse favors a diagnosis of acute liver failure.

Posttherapeutic Morphologic Changes in the Liver

Morphologic changes may also be induced in the liver by the treatment of liver tumors. Indeed, hypertrophy of the remnant liver segments is seen after major liver resection (resection of at least three liver segments). Nonsurgical liver-directed therapy can also cause morphologic changes. In particular, selective intraarterial radiation therapy (or radioembolization) can result in significant changes with marked atrophy

of the treated liver and hypertrophy of the contralateral liver (Fig 7). Selective intraarterial radiation therapy delivers radiolabeled microspheres to malignant liver tumors via the hepatic arteries. This technique is used for the treatment of hepatocellular carcinoma, liver metastases, and cholangiocarcinoma. The increase in size in the nontreated liver regions is similar but slower to that observed with portal vein embolization (20,21). These changes may increase resectability as future liver remnant liver volume is increased, and selective intraarterial radiation therapy can be used as a bridge to major resection, stimulating hypertrophy in the contralateral lobe. Signs of portal hypertension with splenomegaly are found in some patients. It is easy for radiologists and clinicians to recognize this entity based on the patient's history.

Figure 5

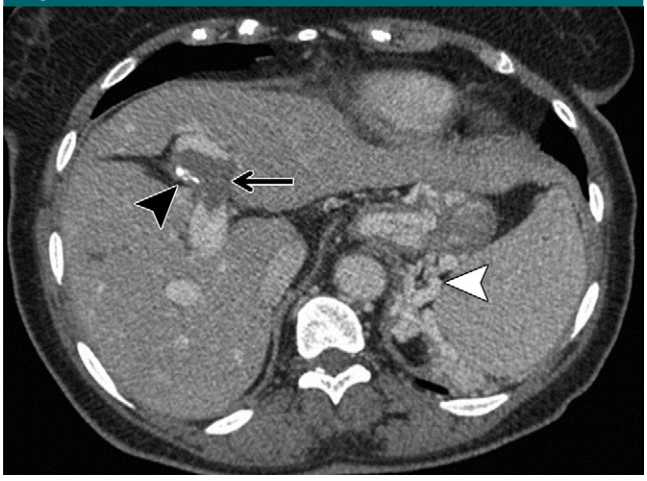

Figure 5: Axial contrast-enhanced CT image in a 69-year-old man with morphologic changes of the liver secondary to obliterative portal venopathy. Portal venous phase image shows right atrophy of the liver. The left portal branch is obstructed (arrow). Note the mural calcifications (black arrowhead), which are suggestive of the diagnosis. Signs of portal hypertension are seen (splenomegaly and portocaval collaterals [white arrowhead]).

Is the Tumor Intrahepatic or Extrahepatic?

Extrahepatic tumors can mimic intrahepatic ones. The larger the tumor the more difficult it is to determine its origin. This is true in many different parts of the body including extrahepatic and intrahepatic tumors. Intrahepatic tumors are easy to identify when they are completely surrounded by the liver parenchyma, but this distinction is much more difficult in tumors adjacent to the liver capsule: Are they intra- or extrahepatic? As a general rule, when the liver parenchyma is not interrupted and when a spur of liver parenchyma is located outside the tumor, it is definitely intrahepatic (Fig 8). Further details are shown in Figure E4 (online). On the contrary, when the liver parenchyma is compressed and displaced with a fat plane between the tumor and the liver parenchyma, the tumor is clearly extrahepatic. These signs have been described in the literature as a "positive embedded organ" (if an organ is embedded in the periphery of a larger mass, the mass probably originates from

Figure 6

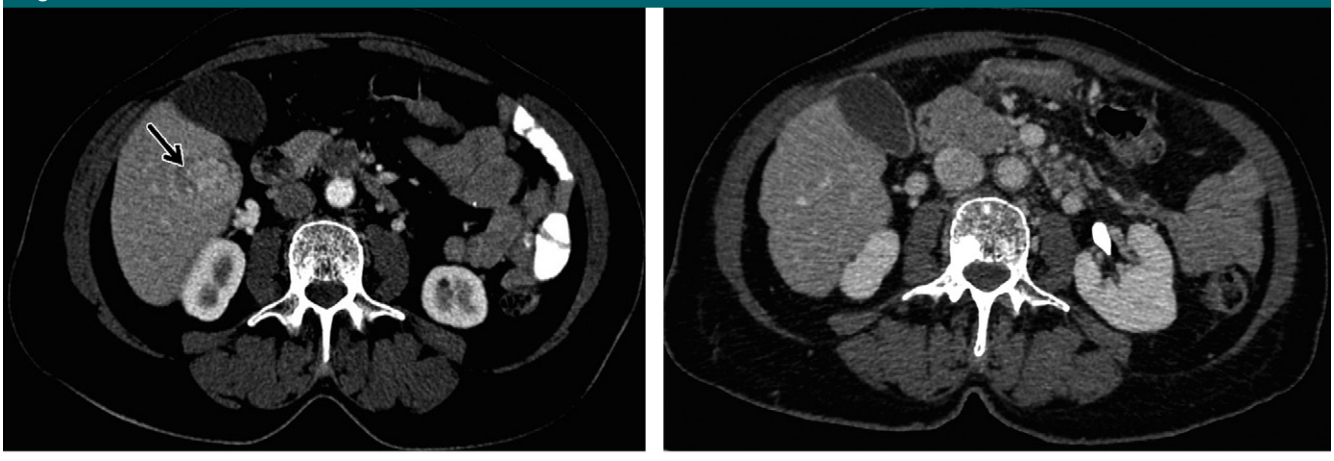

a. b.

Figure 6: Images in a 65-year-old woman with breast cancer and liver metastases. **(a)** Axial contrast-enhanced CT image at the portal venous phase shows one liver metastasis in the right liver (arrow). **(b)** Several years later after multiple cycles of systemic chemotherapy and targeted therapy, contrast-enhanced CT image at the portal venous phase shows nodular liver surface known as pseudocirrhosis.

Figure 7

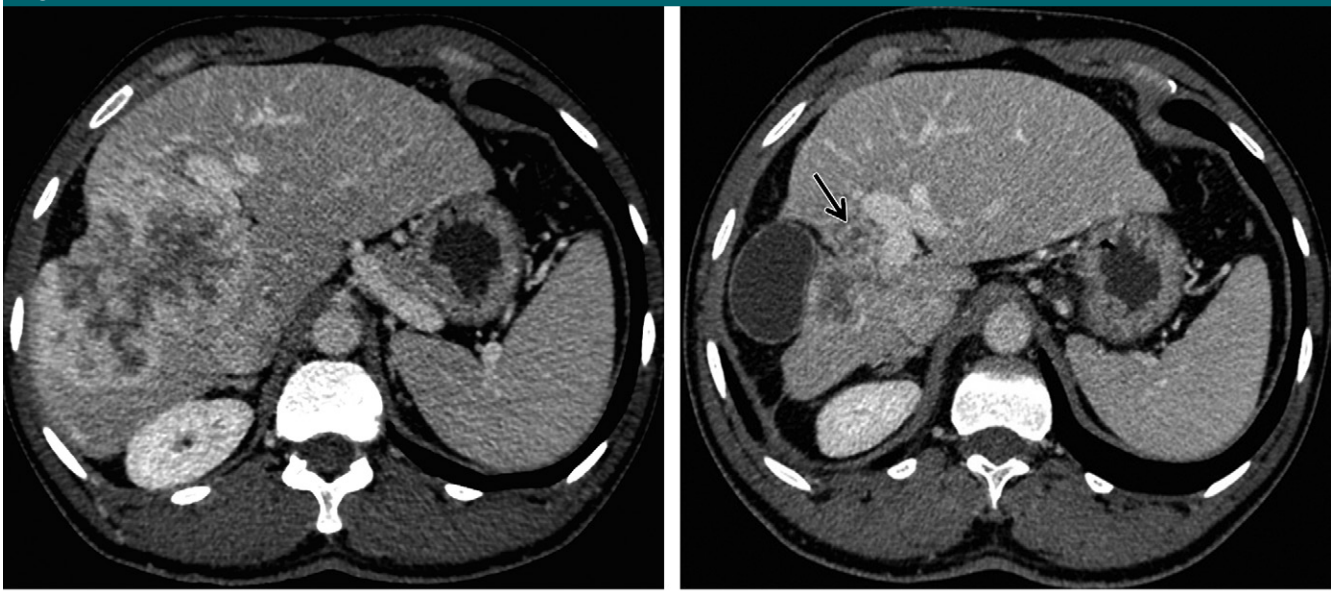

a. b.

Figure 7: Axial contrast-enhanced CT images in a 39-year-old man with intrahepatic cholangiocarcinoma treated with selective intrahepatic radiation therapy (also called radioembolization). **(a)** Portal venous phase image shows the tumor in the right liver, which enhances over time. **(b)** Portal venous phase image obtained 18 months later shows tumor shrinkage (arrow) and right atrophy of the liver. Note the compensatory contralateral hypertrophy.

Figure 8

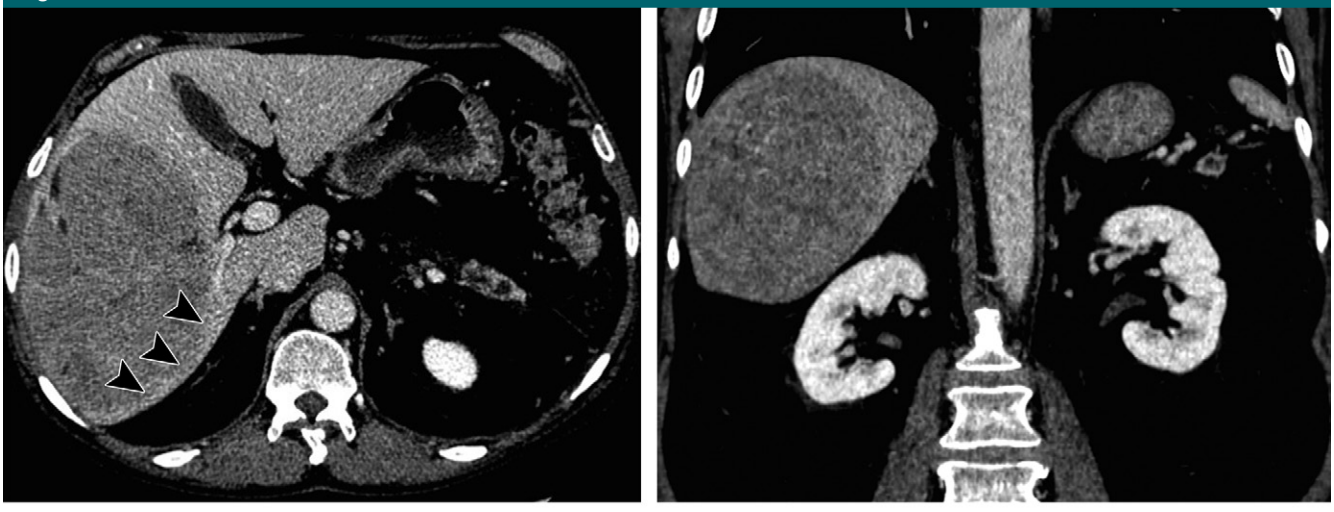

a. b.

Figure 8: CT images in a 59-year-old man with large hepatocellular carcinoma in the right liver. **(a)** Axial contrast-enhanced image in the portal venous phase shows hypoattenuation on the portal venous phase. On arterial phase images (not shown), the tumor was slightly hypervascular. Liver parenchyma is embedded in the periphery of the tumor (arrowheads). **(b)** Coronal contrast-enhanced image at the portal venous phase shows the intrahepatic location. Note absence of displacement of the right kidney.

that organ) and a "negative embedded organ" (if an organ is compressed to the periphery of a solid mass, the mass does not originate from that organ) (22). However these findings may be lacking and in this situation it is helpful to identify the location of the tumor center: If it is outside the liver, the tumor is probably extrahepatic and vice versa. The arterial supply of the tumor is also an important source of information. Indeed it is much easier in hyper-

Figure 9

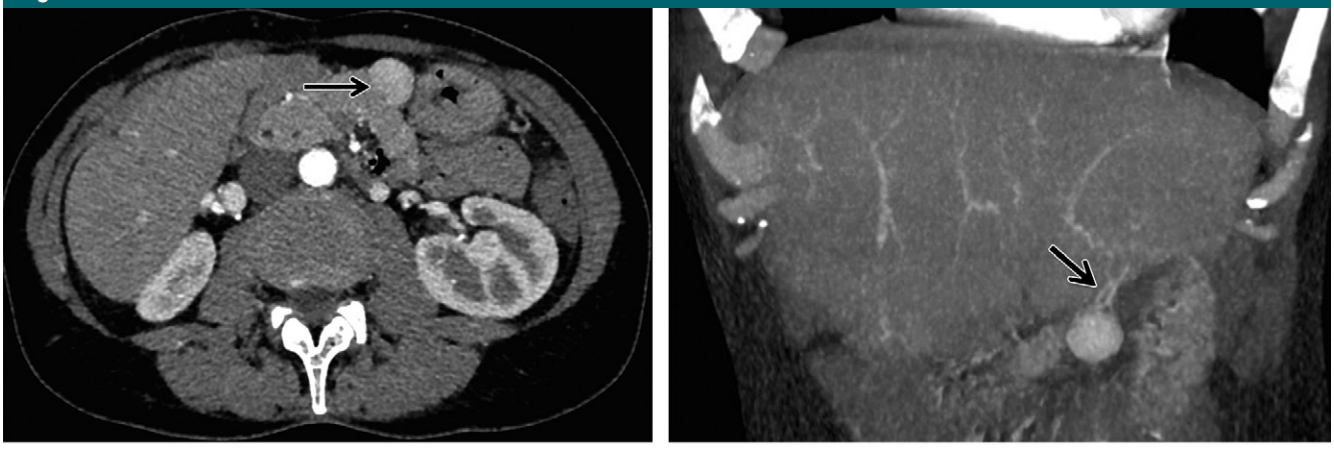

a. b.

Figure 9: CT image in a 58-year-old woman with pedunculated focal nodular hyperplasia. **(a)** Axial contrast-enhanced image at the arterial phase shows a hypervascular lesion lying anteriorly to the pancreas (arrow). No connection is seen with the liver. **(b)** Coronal oblique reconstructed contrast-enhanced image at the arterial phase shows that the lesion is supplied by hepatic arteries (arrow) confirming the hepatic origin.

Figure 10

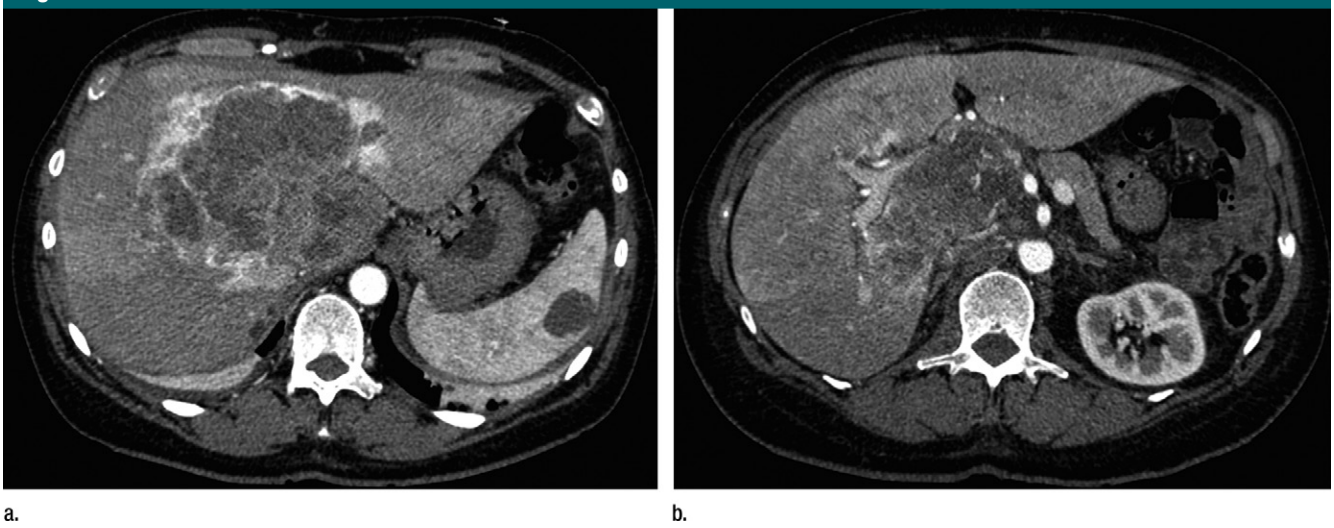

a. b.

Figure 10: **(a, b)** Axial contrast-enhanced CT images obtained at different levels images in a 58-year-old woman with leiomyosarcoma of the IVC. The arterial phase images show a hypervascular lesion that mimics intrahepatic tumor.

vascular tumors than in hypovascular ones. An arterial supply that originates from the hepatic arteries suggests that the tumor originates in the liver, and this finding is very helpful in pedunculated tumors (Fig 9). Further details are shown in Figure E5 (online).

Large tumors can displace vessels, and vascular distortion can be a helpful diagnostic clue. A large tumor arising from the right liver can increase the distance between the right anterior and the right posterior portal branches, while large extrahepatic tumors displace vessels differently. Three main landmarks should be carefully analyzed in large tumors of the right upper quadrant: the IVC, the right portal bifurcation, and the right kidney. In large tumors arising from the IVC (mostly leiomyosarcoma), the lumen of the retrohepatic portion of IVC becomes imperceptible while upstream the IVC is dilated, the tumor is centered on the IVC (Fig 10), and venous collaterals may be depicted subcutaneously and in vertebral pathways (23). Further details are shown in Figure E6 (online). Leiomyosarcomas are slow-growing, well-defined, encapsulated tumors and initially compress the liver parenchyma, but true hepatic invasion may be seen in advanced tumors (24). Large tumors arising from the retroperitoneal space, such as tumors from the adrenal gland, displace the right

Figure 11

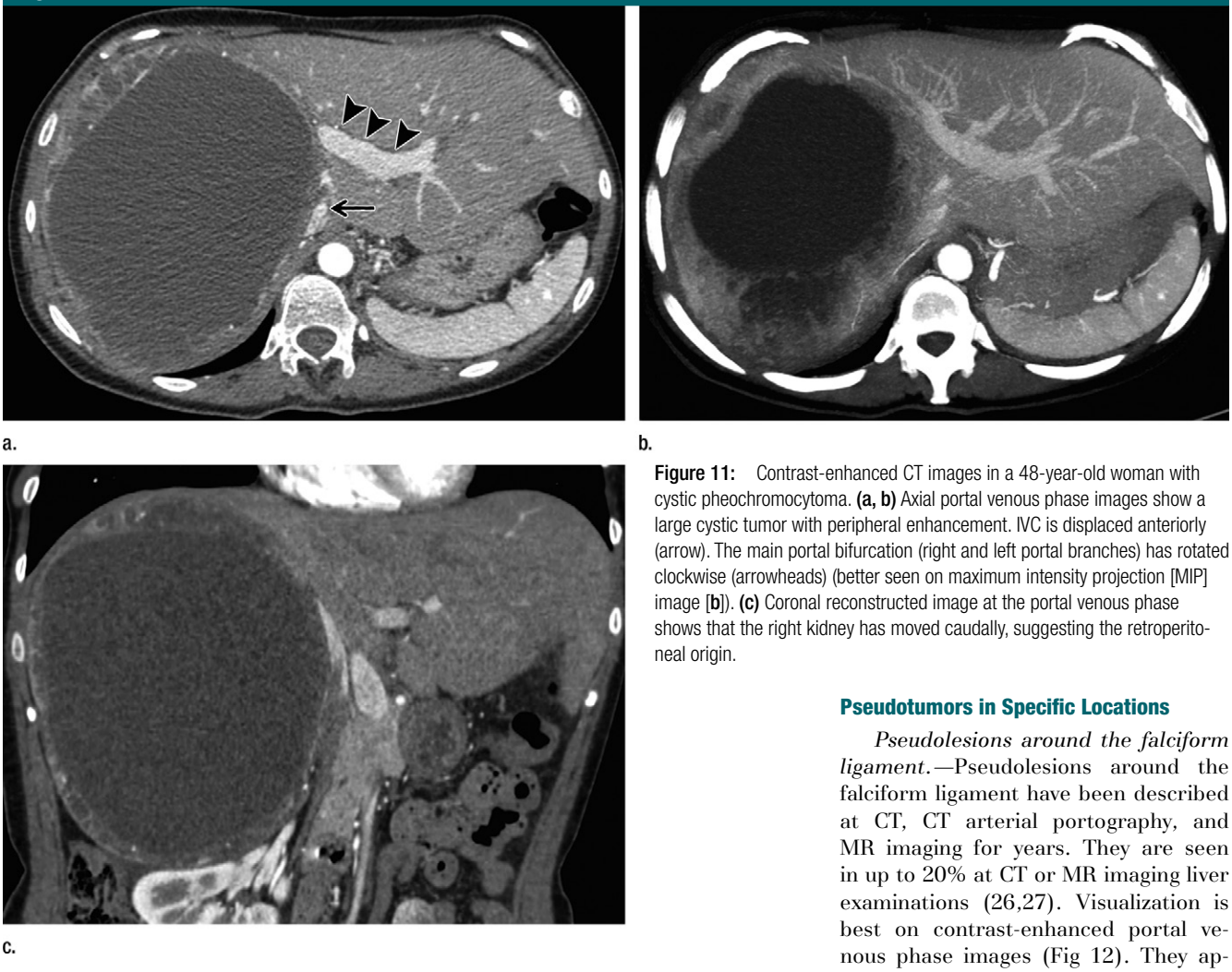

Figure 11: Contrast-enhanced CT images in a 48-year-old woman with cystic pheochromocytoma. **(a, b)** Axial portal venous phase images show a large cystic tumor with peripheral enhancement. IVC is displaced anteriorly (arrow). The main portal bifurcation (right and left portal branches) has rotated clockwise (arrowheads) (better seen on maximum intensity projection [MIP] image [**b**]). **(c)** Coronal reconstructed image at the portal venous phase shows that the right kidney has moved caudally, suggesting the retroperitoneal origin.

liver anteriorly as well as the IVC (Fig 11). Further details are shown in Figure E7 (online). The main portal bifurcation (right and left portal branches) rotates clockwise. Finally the right kidney moves caudally. Indeed, multiplanar reconstructed CT and MR imaging are crucial in this setting.

Besides the large tumors, another challenge is distinguishing capsular implants from true intrahepatic metastases. In a hospital with a large gynecologic-oncology practice, this problem arises regularly because the peritoneum is the most common metastatic site of ovarian cancer. Peritoneal carcinomatosis appears as soft-attenuating plaques or masses. Imaging features that suggest peritoneal origin are the preservation of well-defined lesion–liver interface, the presence of a fatty layer, ascites, and presence of peritoneal implants in other locations. Peritoneal implants are usually hyperintense on both T2-weighted and diffusion-weighted images with low apparent diffusion coefficient values (25).

The Mimics of Intrahepatic Tumors

Focal liver lesions are not necessarily tumors and may be lesions with a pseudotumoral appearance. They will be presented according to their main imaging features: location and imaging characteristics.

Pseudotumors in Specific Locations

Pseudolesions around the falciform ligament.—Pseudolesions around the falciform ligament have been described at CT, CT arterial portography, and MR imaging for years. They are seen in up to 20% at CT or MR imaging liver examinations (26,27). Visualization is best on contrast-enhanced portal venous phase images (Fig 12). They appear as a focal low attenuation or signal intensity on CT or MR images and can also be identified at the arterial phase. These lesions are more rarely seen during the equilibrium phase (28). The mean size is 9 mm and they are more often observed in segment 4 than in the left liver lobe. Although the low attenuation on CT images or low signal intensity on contrast-enhanced MR images adjacent to the falciform ligament was initially thought to be due to focal fat, it is probably related to anomalous venous drainage, because most patients have no signal intensity loss on opposed-phase MR images (27). Moreover, an inferior vein of Sappey (which drains venous blood flow from the anterior part of the abdominal wall into

Figure 12

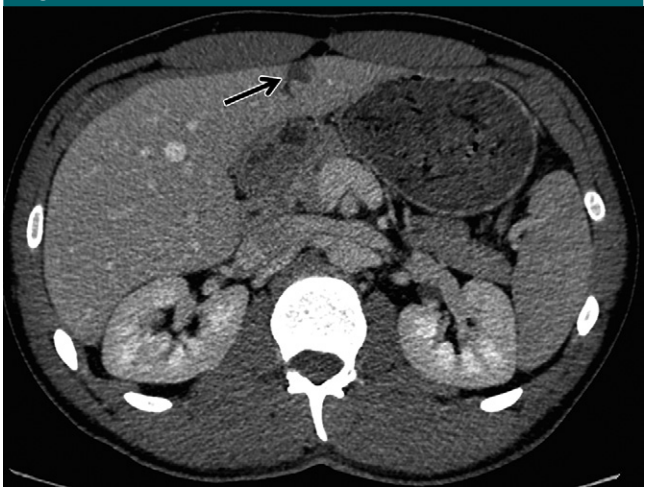

Figure 12: Image in a 34-year-old man with pseudolesion around falciform ligament. Axial contrast-enhanced CT at the arterial phase (not shown) and portal venous phase showed a low attenuation area (arrow) on both phases.

the liver) is often encountered in these pseudolesions (26).

Pseudolesion in the posterior part of segment 4.—A focal liver lesion located in the posterior part of segment 4 initially suggests focal fatty sparing or focal steatosis. Liver steatosis is common and takes on many forms at imaging. It may be diffuse and is easy to recognize. More difficult cases include diffuse steatosis with focal areas of sparing or focal areas of fatty deposits in an otherwise normal liver. Interestingly, the posterior part of segment 4 is the most common location of pseudolesions related to steatosis. Abnormal venous drainage was suspected years ago as the cause for this finding based on CT arterial portography, which often showed lack of enhancement of the posterior part of segment 4, suggesting that the venous supply to this territory did not come directly from the portal vein, but perhaps from the gastric vein or duodenopancreatic venous arcade (29–31). Later, the "venous theory" was modified by the "insulin theory," which has similarly been described in patients with hepatic steatosis who are receiving intraperitoneal insulin (32,33). In these patients, concentrations of insulin, which stimulates the conversion of glucose to fatty acids, vary considerably in the portal vein tributaries. This explains why aberrant right gastric veins (with low insulin concentrations) that drain directly into segment 4 result in focal fatty sparing in that segment (Fig 13). Conversely, aberrant duodenopancreatic arcades (with high insulin concentrations), which drain directly into segment 4, result in focal fatty steatosis (Fig 14).

Pseudolesions around the gallbladder.—In patients with steatosis, focal fatty sparing may be seen around the gallbladder fossa in segments 4 and 5. Interestingly, these pseudolesions are much more frequent in patients with an intact gallbladder than in those who have undergone cholecystectomy (78% versus 33%) (34). Focal fatty sparing around the gallbladder is also probably related to venous drainage because there are almost always small cystic veins (with low insulin concentrations) that drain directly into the liver and are interrupted by cholecystectomy.

Arterially Enhanced Pseudotumors

Most hyperenhancing tumors on arterial-phase contrast-enhanced images are either malignant (hepatocellular carcinoma) or benign hepatocellular lesions such as focal nodular hyperplasia, hepatocellular adenoma, and less frequently nodular regenerative hyperplasia. Very few hypervascular tumors are metastatic; the most common of these are neuroendocrine liver metastases. Nevertheless there are hypervascular pseudotumors of the liver that are often misdiagnosed as true tumors.

Hepatic arterioportal shunts.—Multiphasic CT and MR imaging have been shown to be very useful for the detection and characterization of liver tumors. On the other hand, they often reveal nontumoral anomalies such as hepatic arterioportal shunts. Hepatic arterioportal shunts are communications between the hepatic artery and the portal venous system at different levels: transinusoidal, transvasal, or transtumoral and may be due to various causes, most commonly cirrhosis, tumors, inflammation, and trauma (35). Occlusion of the small hepatic venules and retrograde filling of portal flow by arterioportal anastomosis is the suggested mechanism of hepatic arterioportal shunts in cirrhosis. Arterioportal shunts are seen as a transient increase in enhancement of the parenchyma during the arterial phase on contrast-enhanced CT or MR images with early enhancement of the corresponding portal vein branch (Fig 15). Further details are shown in Figure E8 (online). Indeed, these hypervascular lesions which develop on cirrhosis can mimic hepatocellular carcinoma. Certain imaging features are highly suggestive of hepatic arterioportal shunts. First, increased hepatic parenchymal enhancement predominates on the periphery of the liver and is usually small and wedge-shaped with a straight margin corresponding to lobar, segmental, or subsegmental landmarks. Second, the altered parenchyma returns to normal or nearly normal during the portal venous and delayed phases, which is different from typical hepatocellular carcinoma. Third, there is usually no focal abnormal signal intensity in the region of hyperenhancement on unenhanced T1- and T2-weighted MR images. Recognition of wedge-shaped enhancement is not always easy on axial CT or MR images and multiplanar reconstruction images are helpful. However, hepatic

Figure 13

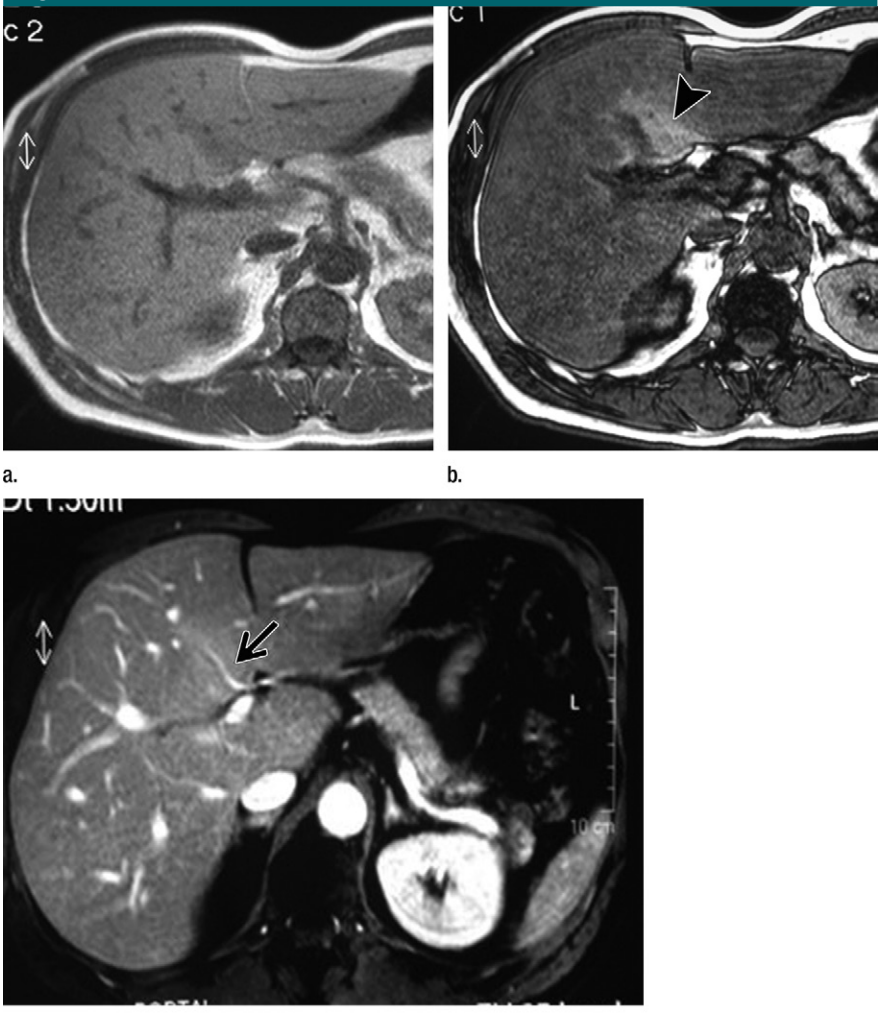

Figure 13: MR images in a 45-year-old man with focal fatty sparing in segment 4. **(a)** In- and **(b)** opposed-phase GRE T1-weighted images (236/2.2 and 4.4; flip angle, 80°; section thickness, 4 mm) show drop of signal intensity in the liver on opposed-phase image related to steatosis. Focal fatty sparing is seen in the posterior part of the segment 4 (arrowhead). **(c)** On contrast-enhanced GRE T1-weighted image (4.5/2.2; flip angle, 10°; section thickness, 4 mm) obtained at the portal phase, a right gastric vein enters directly in segment 4 (arrow).

arterioportal shunts may also be atypical with nodular enhancement and slightly hyperintense T2-weighted images (36,37). In difficult cases, gadoxetic acid–enhanced hepatocyte-phase MR imaging can help confirm the diagnosis of hepatic arterioportal shunts. Very few (5%–15%) are hypointense during the hepatocyte phase, and in these cases, the level of signal intensity is not as low as hepatocellular carcinoma (38,39).

Obstruction of the superior vena cava.—During chronic obstruction of the superior vena cava, collateral pathways develop to maintain venous drainage. In particular, the cavoportal collateral pathway diverts the flow from the superior vena cava to the portal vein on two different tracks: caval-superficial-umbilical-portal and caval-mammary-phrenic–hepatic capsule–portal (40). These collaterals are clearly visualized on contrast-enhanced CT and MR images and may be associated with increased enhancement in the liver (Fig 16) (a so-called "hot spot" on nuclear medicine images) mimicking hypervascular tumors. This increased enhancement of the liver can be seen in up to 29% of the patients with obstruction of the superior vena cava (41). Besides visualization of the venous collaterals, the location of increased enhancement helps identify it as a vascular abnormality because it is mainly found in the anterior part of segment 4 but can also be seen in the subdiaphragmatic portion of the liver (42).

Intrahepatic splenosis.—Intrahepatic splenosis is autotransplantation of splenic tissue in the liver, which usually develops after splenic injury (trauma or surgery). The disrupted splenic fragments acquire a vascular supply and may regrow. Most of the literature has reported misdiagnosis of this entity as hepatocellular carcinoma, neuroendocrine liver metastases, or hepatocellular adenoma because intrahepatic splenosis shows increased enhancement on CT or MR images during the arterial phase (Fig 17) (43–45). Further details are shown in Figure E9 (online). Unfortunately, performing gadoxetic acid–enhanced hepatocyte-phase MR imaging does not solve the problem because intrahepatic splenosis is hypointense during the hepatospecific phase. The keys to diagnose intrahepatic splenosis are knowledge of splenic injury, the subcapsular location of the lesion (mostly in the left liver lobe), and the association with other hypervascular intraperitoneal lesions. If intrahepatic splenosis is suspected, technetium-99m–labeled red blood cell scintigraphy should be performed to confirm the diagnosis.

Fibrous Pseudotumors

Fibrous pseudotumors are predominantly fibrous and enhance during the equilibrium phase or later at contrast-enhanced CT imaging, and during delayed-phase MR imaging using non-hepatospecific contrast agents. Fibrous pseudotumors do not enhance on hepatocyte-phase MR images using hepatospecific contrast agents because of the

Figure 14

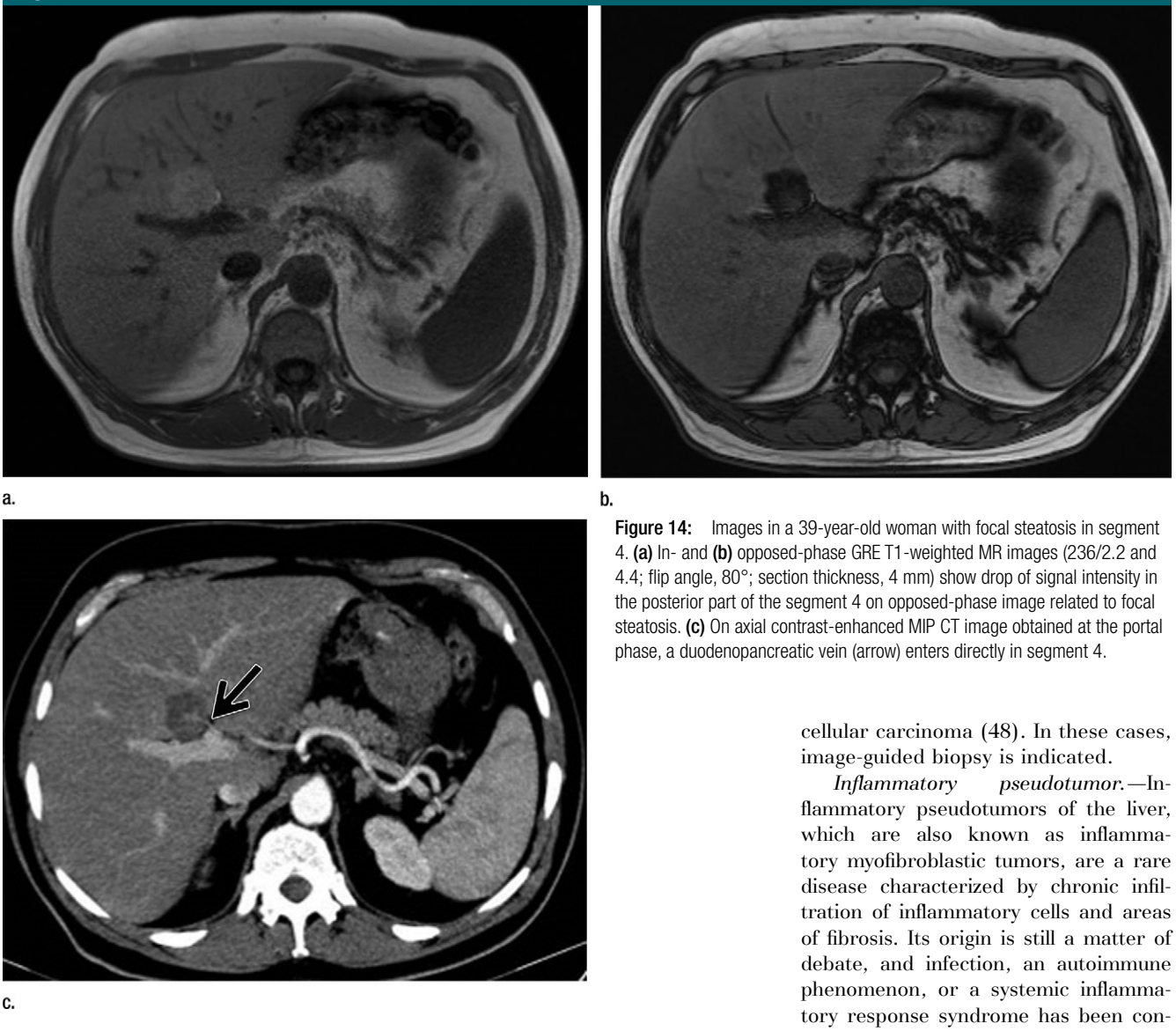

Figure 14: Images in a 39-year-old woman with focal steatosis in segment 4. **(a)** In- and **(b)** opposed-phase GRE T1-weighted MR images (236/2.2 and 4.4; flip angle, 80°; section thickness, 4 mm) show drop of signal intensity in the posterior part of the segment 4 on opposed-phase image related to focal steatosis. **(c)** On axial contrast-enhanced MIP CT image obtained at the portal phase, a duodenopancreatic vein (arrow) enters directly in segment 4.

lack of functioning hepatocytes in these lesions.

Focal confluent fibrosis.—Focal confluent fibrosis is usually found in patients with cirrhosis (mostly alcoholic) and less often in patients with primary sclerosing cholangitis or autoimmune chronic hepatitis. The hepatic parenchyma is replaced by focal fibrosis. Typical imaging findings differ from hepatocellular carcinoma because focal fibrosis usually does not enhance during the arterial phase but does enhance during delayed phase CT or MR imaging with nonhepatospecific contrast agents (Fig 18). Focal confluent fibrosis is moderately hyperintense on T2-weighted MR images (46). Moreover, certain findings strongly suggest this entity: *(a)* specific location, because most cases are found in segments 4, 7, or 8, *(b)* capsular retraction or focal flattening of the capsule (observed in 75% of cases), *(c)* wedge shape, and *(d)* trapped vessels (15%) (47). Nevertheless, focal confluent fibrosis lesions may not be retracted during initial imaging and may even enhance during the arterial phase possibly related to associated inflammation, mimicking hepatocellular carcinoma (48). In these cases, image-guided biopsy is indicated.

Inflammatory pseudotumor.—Inflammatory pseudotumors of the liver, which are also known as inflammatory myofibroblastic tumors, are a rare disease characterized by chronic infiltration of inflammatory cells and areas of fibrosis. Its origin is still a matter of debate, and infection, an autoimmune phenomenon, or a systemic inflammatory response syndrome has been considered. Inflammatory pseudotumors of the liver are often misdiagnosed as intrahepatic cholangiocarcinoma, atypical hepatocellular carcinoma, or hepatic metastasis. Because this is a benign lesion it can be managed conservatively, so it is important to recognize the features of this entity on imaging studies. Inflammatory pseudotumors of the liver commonly manifest as large, solitary masses and mainly occur in the right lobe. They are usually ill defined and hypoattenuating on unenhanced CT images and show peripheral enhancement during the arterial phase followed by central and

Figure 15

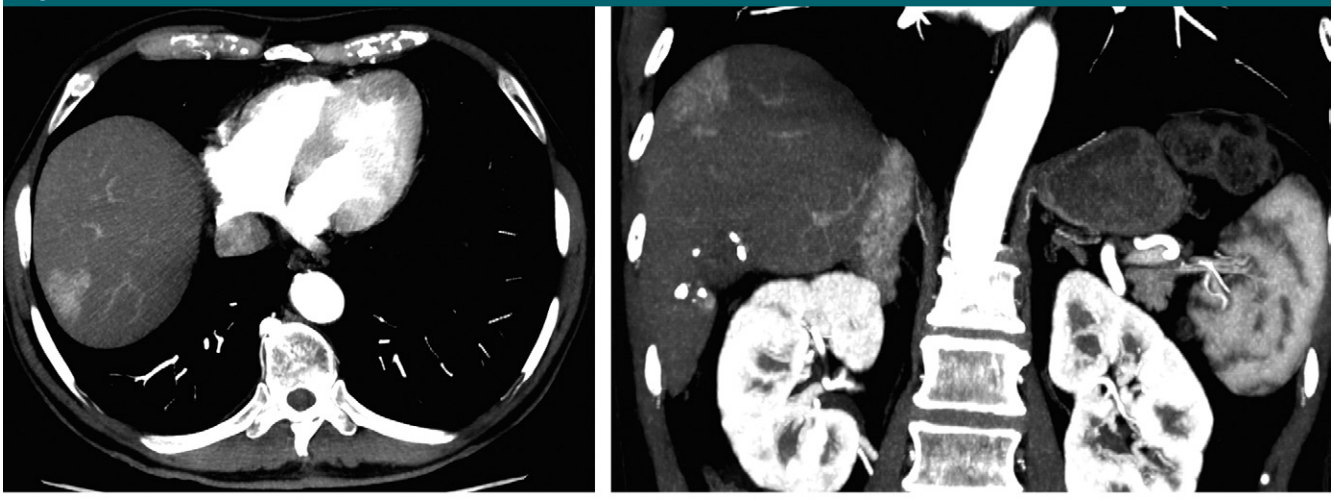

a. b.

Figure 15: Images in a 69-year-old man with arteriovenous shunt diagnosed during the follow-up of alcoholic cirrhosis. MIP **(a)** axial and **(b)** coronal contrast-enhanced CT images at the arterial phase show a peripheral increased enhancement of the liver with a wedge-shaped appearance.

Figure 16

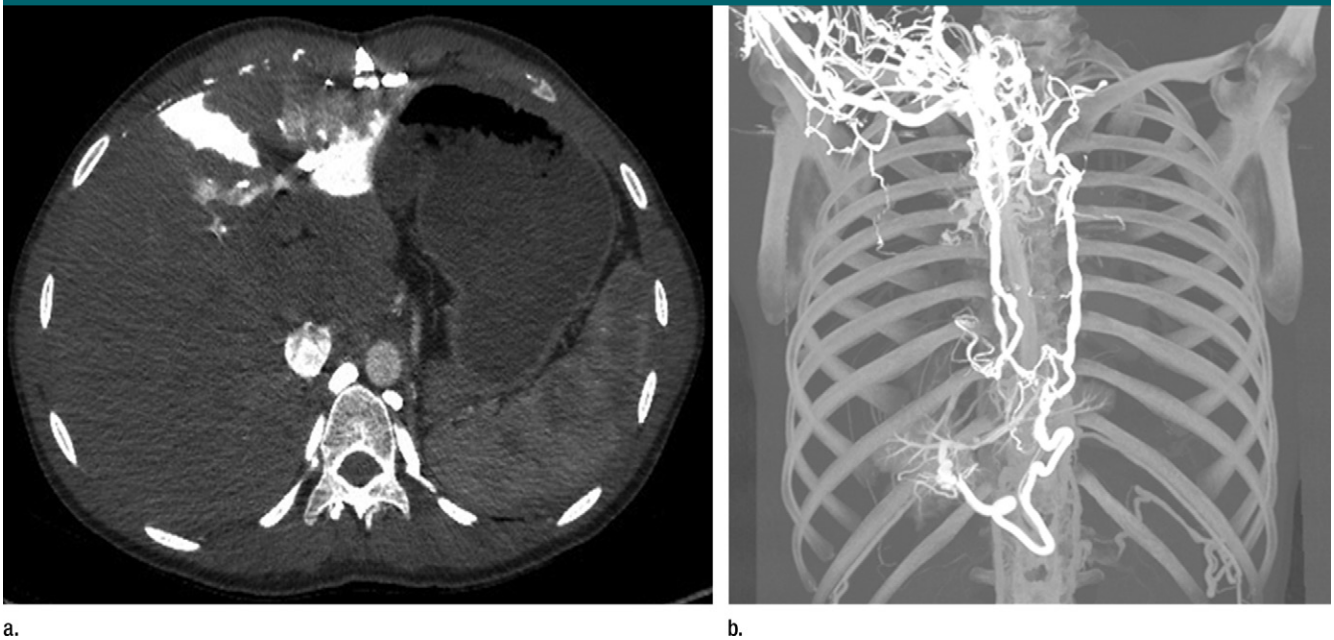

a. b.

Figure 16: Images in a 42-year-old man with complete obstruction of the superior vena cava causing pseudolesion in segment 4. **(a)** Axial contrast-enhanced CT image at the arterial phase shows increased enhancement in the anterior part of segment 4. **(b)** Coronal MIP CT image nicely demonstrates the caval-mammary-phrenic–hepatic capsule–portal collaterals.

heterogeneous enhancement during the portal venous and equilibrium phases (49). Inflammatory pseudotumors of the liver are hypointense on T1- and moderately hyperintense on T2-weighted MR images. Further details are shown in Figure E10 (online). Portal vein obliteration is an interesting associated finding, which is common at pathologic examination but rarer at imaging. Indeed, imaging findings are not specific but are an indication for liver biopsy, which typically shows chronic infiltration of various inflammatory cells (plasma cells, lymphocytes, neutrophils, and eosinophils) and fibrous stroma. A very uncommon pattern is a perihilar inflammatory pseudotumor. In these cases, patients mani-

Figure 17

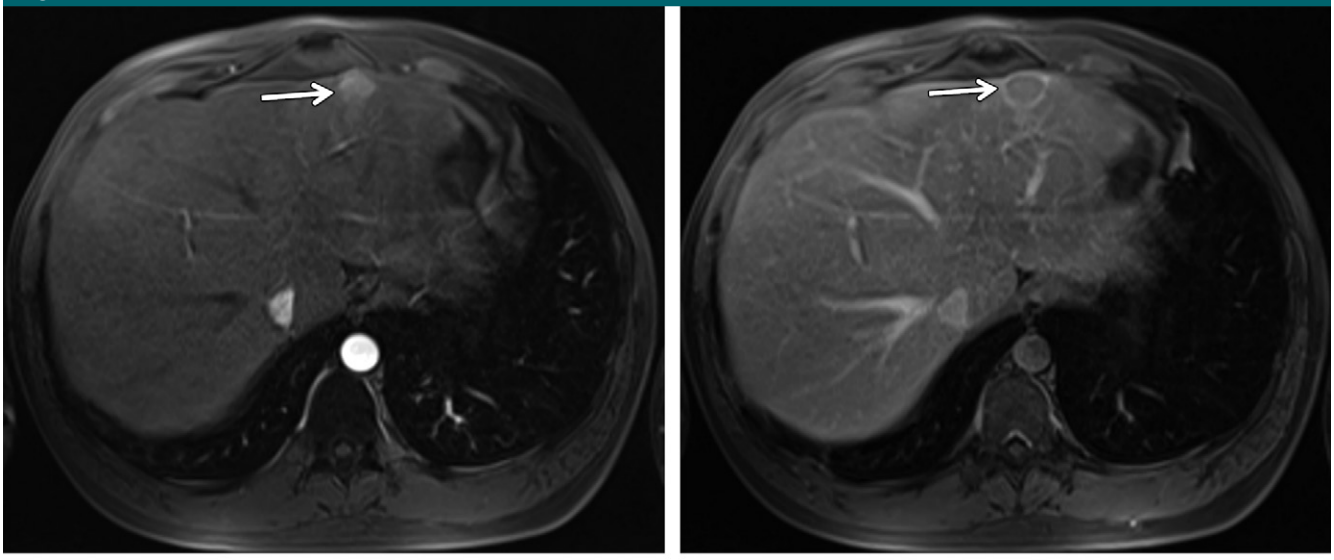

a. b.

Figure 17: Intrahepatic splenosis misdiagnosed as hepatocellular carcinoma in a 51-year-old man with chronic viral hepatitis. This patient had a history of splenectomy. On fat-suppressed fast SE T2-weighted MR image (not shown), the peripheral lesion of the left liver lobe is moderately hyperintense. **(a, b)** On T1-weighted images (4.5/2.2; flip angle, 10°; section thickness, 4 mm), the lesion is hypointense on unenhanced images (not shown), **(a)** enhances (arrow) on the arterial phase image, and **(b)** is isointense on the delayed phase image. A hyperenhancing rim (arrow) is seen on the delayed phase image.

Figure 18

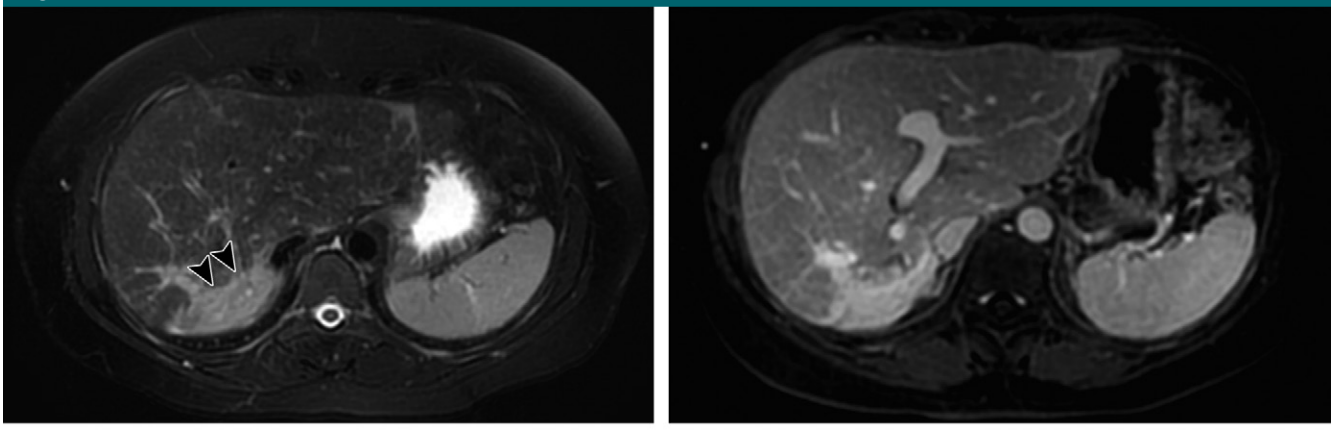

a. b.

Figure 18: Focal confluent fibrosis in a 38-year-old woman with autoimmune cirrhosis. **(a)** Fat-suppressed fast SE T2-weighted MR image (2500–8000/90; flip angle, 90°; section thickness, 4 mm) shows a strongly hyperintense area in the right liver (arrowheads). At T1-weighted imaging (4.5/2.2; flip angle, 10°; section thickness, 4 mm), the lesion is strongly hypointense on unenhanced images, is isointense on arterial phase images (not shown), and **(b)** is strongly hyperintense on delayed phase image using non-hepatospecific MR contrast agent. Such enhancement corresponds to extensive fibrosis. Note also the atrophy of the right liver.

fest jaundice and cholangitis mimicking hilar cholangiocarcinoma (50).

Multiple Pseudotumors Simulating Liver Metastases

Pseudotumoral nodular steatosis.—In rare instances, liver steatosis appears as multiple lesions distributed throughout the liver parenchyma mimicking liver tumors and especially liver metastases. The lesions are hyperechoic and homogeneous at ultrasonography, hypoattenuating during all CT phases, with enhancement that is theoretically parallel to that of the liver. Drops in signal intensity on opposed-phase T1-weighted MR images confirm the presence of fat in lesions. Findings suggesting pseudotumoral nodular steatosis are the presence of multiple, small (less than 2 cm) lesions and the

Figure 19

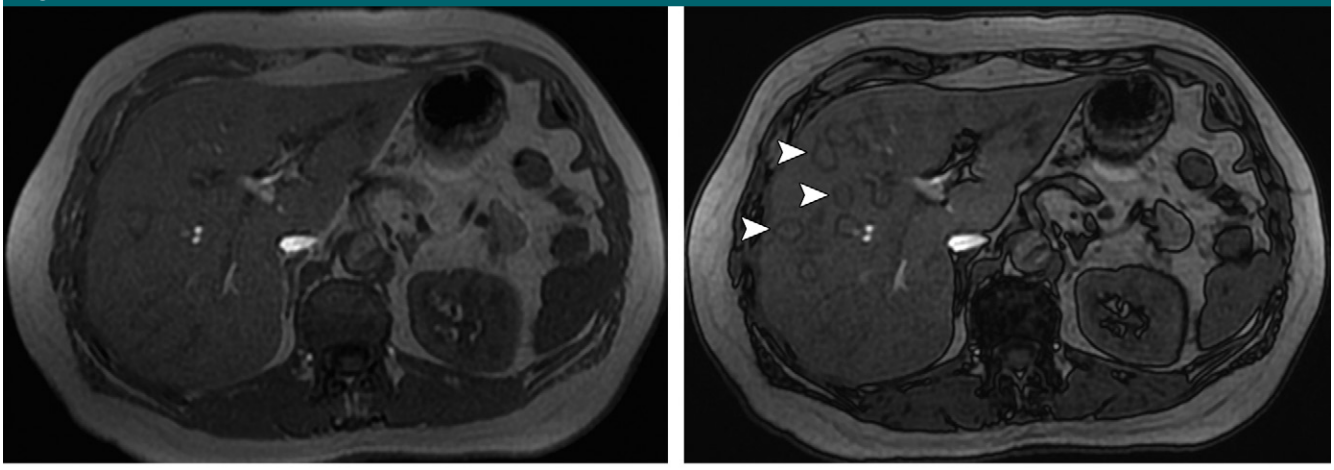

a. b.

Figure 19: Images in a 66-year-old woman with pseudotumoral steatosis. **(a)** In- and **(b)** opposed-phase GRE T1-weighted MR images (236/2.2 and 4.4; flip angle, 80°; section thickness, 4 mm) show multiple small-sized lesions that drop in signal intensity on the opposed-phase image related to pseudotumoral steatosis (arrowheads). The presence of a more fatty border on the periphery of the lesions is highly suggestive of pseudotumoral steatosis.

Figure 20

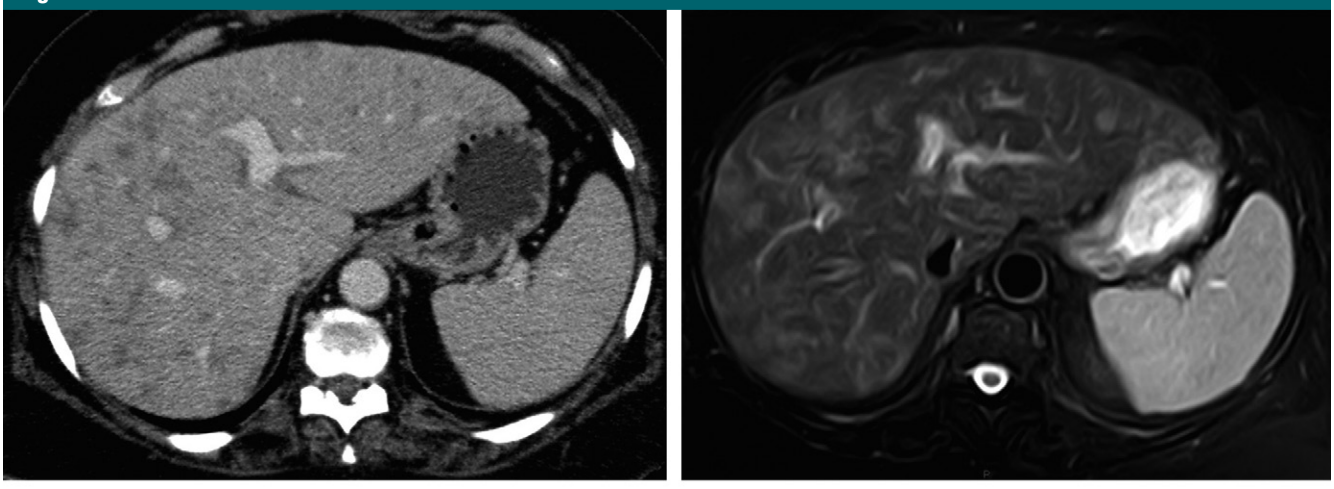

a. b.

Figure 20: Images in a 70-year-old woman with pseudotumoral sarcoidosis. **(a)** The liver is unremarkable at arterial-phase contrast-enhanced CT (not shown) while multiple ill-defined low-attenuation lesions are seen at portal venous phase CT. **(b)** Fat-suppressed fast SE T2-weighted MR image (2500–8000/90; flip angle, 90°; section thickness, 4 mm) shows multiple moderately hyperintense liver lesions.

inconsistent but highly pathognomonic presence of a more fatty border on the periphery of the lesions (Fig 19) (32,51). Further details are shown in Figure E11 (online).

Pseudotumoral granulomatosis.—Liver granulomatosis is common at pathologic examination but is rarely visible at imaging because granulomas are usually microscopic. However pseudotumoral features have been reported with various granulomatous liver diseases, most commonly tuberculosis, sarcoidosis, and brucellosis. There are three different patterns to liver granulomatosis at imaging: miliary, nodular, and multinodular (Fig 20) (52,53). Further details are shown in Figure E12 (online).

Contrast enhancement of lesions is usually absent or weak. Calcifications may be present. There is uptake on fluorodeoxyglucose positron emission tomography images with certain lesions, mimicking malignant tumors. The diagnosis can be extremely difficult in patients with no extrahepatic involvement, and guided biopsy should be proposed in doubtful cases.

Conclusion

This review has highlighted the major pitfalls in liver imaging: the differentiation between cirrhosis and pseudocirrhosis and the distinction between liver tumors and pseudotumors. Most of these pitfalls can be avoided by the careful analysis of all imaging findings in relation to their fit with the clinical background of the patient.

Disclosures of Conflicts of Interest: V.V. disclosed no relevant relationships. **M.L.** disclosed no relevant relationships. **M.R.** disclosed no relevant relationships.

References

1. Ito K, Mitchell DG, Siegelman ES. Cirrhosis: MR imaging features. Magn Reson Imaging Clin N Am 2002;10(1):75–92, vi.
2. Hann LE, Getrajdman GI, Brown KT, et al. Hepatic lobar atrophy: association with ipsilateral portal vein obstruction. AJR Am J Roentgenol 1996;167(4):1017–1021.
3. Schweizer W, Duda P, Tanner S, et al. Experimental atrophy/hypertrophy complex (AHC) of the liver: portal vein, but not bile duct obstruction, is the main driving force for the development of AHC in the rat. J Hepatol 1995;23(1):71–78.
4. Lambotte L, Li B, Leclercq I, Sempoux C, Saliez A, Horsmans Y. The compensatory hyperplasia (liver regeneration) following ligation of a portal branch is initiated before the atrophy of the deprived lobes. J Hepatol 2000;32(6):940–945.
5. Ozaki K, Matsui O, Kobayashi S, et al. Selective atrophy of the middle hepatic venous drainage area in hepatitis C-related cirrhotic liver: morphometric study by using multidetector CT. Radiology 2010;257(3):705–714.
6. Vilgrain V, Condat B, Bureau C, et al. Atrophy-hypertrophy complex in patients with cavernous transformation of the portal vein: CT evaluation. Radiology 2006;241(1):149–155.
7. Valla DC. Primary Budd-Chiari syndrome. J Hepatol 2009;50(1):195–203.
8. Buckley O, O'Brien J, Snow A, et al. Imaging of Budd-Chiari syndrome. Eur Radiol 2007;17(8):2071–2078.
9. Zeitoun D, Brancatelli G, Colombat M, et al. Congenital hepatic fibrosis: CT findings in 18 adults. Radiology 2004;231(1):109–116.
10. Gunay-Aygun M, Font-Montgomery E, Lukose L, et al. Characteristics of congenital hepatic fibrosis in a large cohort of patients with autosomal recessive polycystic kidney disease. Gastroenterology 2013;144(1):112–121.e2.
11. Krishnan P, Fiel MI, Rosenkrantz AB, et al. Hepatoportal sclerosis: CT and MRI appearance with histopathologic correlation. AJR Am J Roentgenol 2012;198(2):370–376.
12. Isabel Fiel M, Thung SN, Hytiroglou P, Emre S, Schiano TD. Liver failure and need for liver transplantation in patients with advanced hepatoportal sclerosis. Am J Surg Pathol 2007;31(4):607–614.
13. Glatard AS, Hillaire S, d'Assignies G, et al. Obliterative portal venopathy: findings at CT imaging. Radiology 2012;263(3):741–750.
14. Young ST, Paulson EK, Washington K, Gulliver DJ, Vredenburgh JJ, Baker ME. CT of the liver in patients with metastatic breast carcinoma treated by chemotherapy: findings simulating cirrhosis. AJR Am J Roentgenol 1994;163(6):1385–1388.
15. Battisti S, Guida FM, Pagliara E, Tonini G, Zobel BB, Santini D. Pseudocirrhosis after anti-EGFR-based neoadjuvant therapy for hepatic metastasis from colon cancer: a different point of view. Clin Colorectal Cancer 2014;13(3):e13–e15.
16. Kang SP, Taddei T, McLennan B, Lacy J. Pseudocirrhosis in a pancreatic cancer patient with liver metastases: a case report of complete resolution of pseudocirrhosis with an early recognition and management. World J Gastroenterol 2008;14(10):1622–1624.
17. Qayyum A, Lee GK, Yeh BM, Allen JN, Venook AP, Coakley FV. Frequency of hepatic contour abnormalities and signs of portal hypertension at CT in patients receiving chemotherapy for breast cancer metastatic to the liver. Clin Imaging 2007;31(1):6–10.
18. Romero M, Palmer SL, Kahn JA, et al. Imaging appearance in acute liver failure: correlation with clinical and pathology findings. Dig Dis Sci 2014;59(8):1987–1995.
19. Poff JA, Coakley FV, Qayyum A, et al. Frequency and histopathologic basis of hepatic surface nodularity in patients with fulminant hepatic failure. Radiology 2008;249(2):518–523.
20. Edeline J, Lenoir L, Boudjema K, et al. Volumetric changes after (90)y radioembolization for hepatocellular carcinoma in cirrhosis: an option to portal vein embolization in a preoperative setting? Ann Surg Oncol 2013;20(8):2518–2525.
21. Vouche M, Lewandowski RJ, Atassi R, et al. Radiation lobectomy: time-dependent analysis of future liver remnant volume in unresectable liver cancer as a bridge to resection. J Hepatol 2013;59(5):1029–1036.
22. Minami M, Ohmoto K, Charnsangavej C, Kawauchi N, Itai A, Sasaki S. Origin of abdominal tumors: useful findings and signs on tomographic imaging [abstract]. Radiology 1996;201(P):491.
23. Webb EM, Wang ZJ, Westphalen AC, Nakakura EK, Coakley FV, Yeh BM. Can CT features differentiate between inferior vena cava leiomyosarcomas and primary retroperitoneal masses? AJR Am J Roentgenol 2013;200(1):205–209.
24. Blum U, Wildanger G, Windfuhr M, Laubenberger J, Freudenberg N, Munzar T. Preoperative CT and MR imaging of inferior vena cava leiomyosarcoma. Eur J Radiol 1995;20(1):23–27.
25. Beranger-Gibert S, Lagadec M, Boulay-Coletta I, et al. Hepatic and perihepatic involvement of female genital diseases and pregnancy: a review. Abdom Imaging 2015;40(5):1331–1349.
26. Genchellac H, Yilmaz S, Ucar A, Dursun M, Demir MK, Yekeler E. Hepatic pseudolesion around the falciform ligament: prevalence, aberrant venous supply, and fatty infiltration evaluated by multidetector computed tomography and magnetic resonance imaging. J Comput Assist Tomogr 2007;31(4):526–533.
27. Macari M, Yeretsian R, Babb J. Assessment of low signal adjacent to the falciform ligament on contrast-enhanced MRI. AJR Am J Roentgenol 2007;189(6):1443–1448.
28. Spelle L, Soyer P, Rondeau Y, Gouhiri M, Scherrer A, Rymer R. Nontumorous hepatic pseudolesion around the falciform ligament: prevalence on gadolinium chelate-enhanced MR examination. AJR Am J Roentgenol 1997;169(3):795–799.
29. Hashimoto M, Heianna J, Tate E, Nishii T, Iwama T, Ishiyama K. Small veins entering the liver. Eur Radiol 2002;12(8):2000–2005.
30. Matsui O, Kadoya M, Yoshikawa J, et al. Aberrant gastric venous drainage in cirrhotic livers: imaging findings in focal areas of liver parenchyma. Radiology 1995;197(2):345–349.
31. Gabata T, Matsui O, Kadoya M, et al. Aberrant gastric venous drainage in a focal spared area of segment IV in fatty liver: demonstration with color Doppler sonography. Radiology 1997;203(2):461–463.
32. Vilgrain V, Ronot M, Abdel-Rehim M, et al. Hepatic steatosis: a major trap in liver imaging. Diagn Interv Imaging 2013;94(7-8):713–727.

33. Nevalainen PI, Kallio T, Lahtela JT, Mustonen J, Pasternack AI. High peritoneal permeability predisposes to hepatic steatosis in diabetic continuous ambulatory peritoneal dialysis patients receiving intraperitoneal insulin. Perit Dial Int 2000;20(6):637–642.

34. Aubin B, Denys A, Lafortune M, Déry R, Breton G. Focal sparing of liver parenchyma in steatosis: role of the gallbladder and its vessels. J Ultrasound Med 1995;14(2):77–80.

35. Choi BI, Lee KH, Han JK, Lee JM. Hepatic arterioportal shunts: dynamic CT and MR features. Korean J Radiol 2002;3(1):1–15.

36. Yu JS, Kim KW, Jeong MG, Lee JT, Yoo HS. Nontumorous hepatic arterial-portal venous shunts: MR imaging findings. Radiology 2000;217(3):750–756.

37. Matsuo M, Kanematsu M, Kondo H, et al. Arterioportal shunts mimicking hepatic tumors with hyperintensity on T2-weighted MR images. J Magn Reson Imaging 2002; 15(3):330–333.

38. Sun HY, Lee JM, Shin CI, et al. Gadoxetic acid-enhanced magnetic resonance imaging for differentiating small hepatocellular carcinomas (< or =2 cm in diameter) from arterial enhancing pseudolesions: special emphasis on hepatobiliary phase imaging. Invest Radiol 2010;45(2):96–103.

39. Motosugi U, Ichikawa T, Sou H, et al. Distinguishing hypervascular pseudolesions of the liver from hypervascular hepatocellular carcinomas with gadoxetic acid-enhanced MR imaging. Radiology 2010;256(1):151–158.

40. Kapur S, Paik E, Rezaei A, Vu DN. Where there is blood, there is a way: unusual collateral vessels in superior and inferior vena cava obstruction. RadioGraphics 2010;30(1):67–78.

41. Siegel Y, Schallert E. Prevalence and etiology of focal liver opacification in patients with superior vena cava obstruction. J Comput Assist Tomogr 2013;37(5):805–808.

42. Sheth S, Ebert MD, Fishman EK. Superior vena cava obstruction evaluation with MDCT. AJR Am J Roentgenol 2010;194 (4):W336–W346.

43. Sato N, Abe T, Suzuki N, et al. Intrahepatic splenosis in a chronic hepatitis C patient with no history of splenic trauma mimicking hepatocellular carcinoma. Am J Case Rep 2014;15:416–420.

44. Leong CW, Menon T, Rao S. Post-traumatic intrahepatic splenosis mimicking a neuroendocrine tumour. BMJ Case Rep 2013 Mar 6;2013.

45. Gruen DR, Gollub MJ. Intrahepatic splenosis mimicking hepatic adenoma. AJR Am J Roentgenol 1997;168(3):725–726.

46. Ohtomo K, Baron RL, Dodd GD 3rd, Federle MP, Ohtomo Y, Confer SR. Confluent hepatic fibrosis in advanced cirrhosis: evaluation with MR imaging. Radiology 1993; 189(3):871–874.

47. Brancatelli G, Baron RL, Federle MP, Sparacia G, Pealer K. Focal confluent fibrosis in cirrhotic liver: natural history studied with serial CT. AJR Am J Roentgenol 2009; 192(5):1341–1347.

48. Baron RL, Peterson MS. From the RSNA refresher courses: screening the cirrhotic liver for hepatocellular carcinoma with CT and MR imaging: opportunities and pitfalls. RadioGraphics 2001;21(Spec No):S117–S132.

49. Park JY, Choi MS, Lim YS, et al. Clinical features, image findings, and prognosis of inflammatory pseudotumor of the liver: a multicenter experience of 45 cases. Gut Liver 2014;8(1):58–63.

50. Deng FT, Li YX, Ye L, Tong L, Yang XP, Chai XQ. Hilar inflammatory pseudotumor mimicking hilar cholangiocarcinoma. Hepatobiliary Pancreat Dis Int 2010;9(2):219–221.

51. Prasad SR, Wang H, Rosas H, et al. Fat-containing lesions of the liver: radiologic-pathologic correlation. RadioGraphics 2005;25(2): 321–331.

52. Yu RS, Zhang SZ, Wu JJ, Li RF. Imaging diagnosis of 12 patients with hepatic tuberculosis. World J Gastroenterol 2004;10(11):1639–1642.

53. Giovinale M, Fonnesu C, Soriano A, et al. Atypical sarcoidosis: case reports and review of the literature. Eur Rev Med Pharmacol Sci 2009;13(Suppl 1):37–44.